Presented at GNSS 2004
The 2004 International Symposium on GNSS/GPS

Sydney, Australia
6–8 December 2004

Acquisition Performance Analysis for BOC Modulated Signals

Maurizio Fantino, Fabio Dovis, Letizia Lo Presti
Politecnico di Torino
Electronics Department
c.so duca degli Abruzzi 24
10129 Torino - Italy
Tel: +39-011 227 6415
Fax: +39-011 564.4099
Email: name.surname@polito.it

Jinling Wang
School of Surveying & Spatial Information Systems
University of New South Wales
Sydney NSW Australia
Location: EE Building 405
Tel: +61 2 9385 4203
Fax: +61 2 9313 7493
Email: jinling.wang@unsw.edu.au

Presenter: Maurizio Fantino

ABSTRACT

The advent of the new European satellite navigation system Galileo and the current study of a new generation of GPS satellites are increasing the interest towards navigation related systems, services and applications. Both the systems foresee improved performances with respect to the present GPS C/A code, mainly achieved by using novel modulation schemes for the signals-In-Space. The Binary Offset Carrier (BOC) modulation, different (and longer) codes, and pilot channels have been proposed as a mean to reduce the mutual interference on common carriers, and also as a way to improve the expected performance. On the receiver side these system design choices have a relevant impact on the receiver architecture which as now to deal with different signals.

One of the core techniques affected by these choices is certainly the acquisition stage, which has the goal to detect the presence of a certain satellite and to provide a rough estimation of the local code alignment and Doppler shift.

This work will address the comparison of the acquisition schemes useful for acquiring the Galileo BOC modulated signals It is well known that several acquisition schemes for CDMA signals can be found in literature; many of them, however, are not suitable for navigation application where the signal to noise ratio is a critical parameter. These algorithms successfully adapted for GPS C/A code in the past must now be reviewed for the BOC modulated signal where the presence of side peaks in the correlation function can increase (if not properly processed) the probability of false alarm of the acquisition stage.

Conventional serial search algorithms and FFT based algorithms on the basis of the system complexity, taking into account the number of quantization levels and acquisition accuracy (in terms of probability of false alarm) for different value of SNR will be studied. In order to compare the various acquisition systems and to identify the schemes that can be successfully used in the acquisition of Galileo signals, a simulation based analysis has been performed in order to identify the best acquisition schemes (and the relative parameters) that can work with the Galileo signals trading the receiver complexity with the expected performance.

KEYWORDS: Galileo, BOC, Serial Search, Parallel Search, Quantization.

1. INTRODUCTION

When a GPS receiver is turned on, a sequence of operation must be ensured before information on the GPS signal can be decoded and the navigation position can be evaluated. After all theses steps the receiver is able to perform the data bit synchronization and demodulate the navigation data. All the sequences from the receiver start up to the detection and signal confirmation are usually called acquisition phase.

Time To First Fix (TTFF) (i.e the time required to have the first estimated position) can be minimized reducing the time required by the acquisition stage. This can be achieved using the approximate time, approximate position of the receiver during the start up process and almanac data (i.e. “hot start”). The receiver can use this information to calculate the elevation angle of each satellite and identify the visible satellites as those whose elevation angle is greater than a specified value. The TTFF can be further reduced if the approximate Doppler shifts of the visible satellite signals are known. This permits the receiver to establish a frequency search pattern in which the most likely frequency of reception is searched first.

Several acquisition schemes for CDMA signals can be found in literature; many of them, however, are designed for personal communications and they work at higher signal-to-noise ratios (SNR) than the values usually guaranteed for GPS and Galileo signals. Many authors do not consider the residual carrier acquisition, but only the code synchronization: this is the case described by Hopkins (1997), Holmes *et al* (1997), for analog receivers.

Other papers do not consider the Doppler frequency shift, which is particularly harmful for GPS and Galileo systems Polydoros (2000), Rappaport (1984), Tae-Hoon (2000), Lee (2001) and Yan (2002) deal with the code acquisition problem in CDMA systems neglecting the Doppler effect on the carrier.

In other cases, finally, the carrier is considered completely acquired before a code rough synchronization, which is impossible for the acquisition of GPS and Galileo signals: examples of this kind of analysis can be found in Delva (2001) and Chang (2000).

In this paper we will consider different acquisition schemes of PRN codes, tailored to the satellite navigation, for the specific Galileo Signal-In-Space (SIS Open Service (OS)) on the L1 carrier, providing a comparative study of their performance.

Section 2 briefly introduces the Galileo specifications for the OS, while the acquisition systems that deal with both code and Doppler frequency shift synchronization are presented in Section 3. In Section 4 these schemes are compared on the basis of simulations. The comparison will be performed with Galileo BOC(1,1) L1 signal parameters and the for all these schemes the analysis of the performance varying the signal quantization level and system complexity is carried out in detail.

2. Galileo SIS Features

Even if the Galileo Programme Phase B has defined the largest part of the Galileo SIS several details are still to be confirmed. According to the SIS specifications the OS signals (i.e., the signal available for free civil applications) should comprise un-encrypted ranging codes and un-encrypted Navigation Data Messages on the E5-A and E5-B carriers and on the B and C channels of the L1 carrier. Table 1 presents the main signal features for the Galileo OS.

Signal Name	Code Length	Chip Rate [MHz]	Data Rate (bit/s)	Bandwidth [MHz]
E5a-I	10230	10.23	50	24
E5a-Q	10230	10.23	No Data	24
E5b-I	10230	10.23	250	24
E5b-Q	10230	10.23	No Data	24
E2-L1-E1-B	8184	2.046	250	40
E2-L1_E1-B	8184	2.046	No Data	40

Table 1 Signal Features for Galileo Open Access Service

The $BOC[f_S, f_C]$ modulation proposed for the Galileo SIS presents features allowing for an improvement of the acquisition and tracking performance, while opening different implementation strategies for the demodulation chain within the receiver, with different complexity costs. The higher rate at which the transition occurs allows for a theoretically better resolution in the time domain. Figure 1 reports a comparison between the correlation function of GPS C/A code and $BOC[1,1]$ SIS.

As previously stated different opportunities are open for the BOC signals demodulation and processing. This is particularly true for the acquisition stage, for which each solution has a different degree of complexity, and thus different performance can be expected, as discussed in the following.

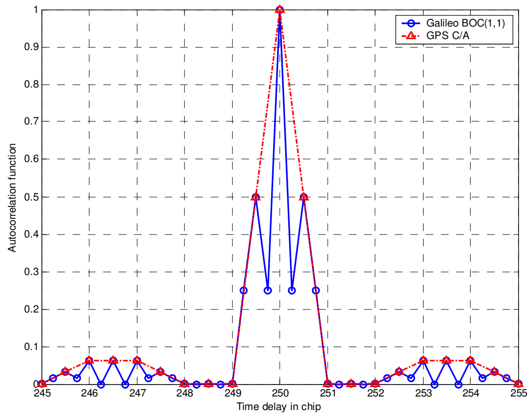

Figure 1 GPS C/A and Galileo BOC(1,1) autocorrelation function comparison

3. Description of different acquisition schemes

3.1 Serial search scheme: infinite-bit ADC with floating point local sinusoids implementation

A basic scheme of a non-coherent acquisition system can be found in Weihua (1995) and is shown in Figure 2: this scheme implements the serial search in time delay and Doppler frequency shift domains and it will be addressed to as *serial search* scheme.

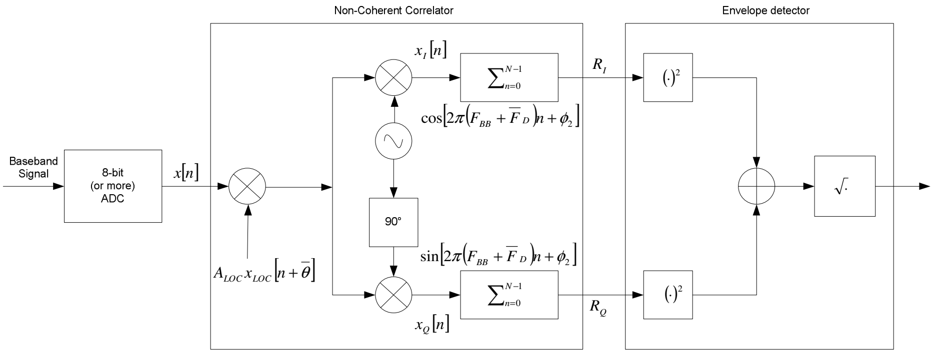

Figure 2 Basic Acquisition Scheme

The input signal after the down-conversion stages and the digitization is expressed by:

$$x[n] = x_C[n] + n_W[n] = A_{IN} x_{IN}[n+\theta]\cos[2\pi(F_{BB}+F_D)(n+\theta)+\phi_1] + n_W[n] \tag{1}$$

where A_{IN} is the useful signal amplitude, x_{IN} is the received PRN code, n_W is a white Gaussian noise with zero mean and variance $\sigma_n^2 = \frac{A_{IN}^2}{2SNR_{IN}}$ and F_{BB} is the baseband frequency after the down conversions of the RF front-end. F_D is the Doppler frequency shift and θ is the received code delay.

The input signal $x[n]$ is multiplied by the local replica of the PRN code $x_{LOC}[n+\overline{\theta}]$, whose delay $\overline{\theta}$ is the estimate of the received satellite code delay; the resulting signal is split into two branches: in the upper one it is multiplied by a local cosine and in the lower branch it is multiplied by a local sine, whose frequencies are the baseband frequency plus the estimate of the Doppler frequency shift $\overline{F}_D$.

The resulting useful signals on the two branches can be expressed as:

$$
\begin{aligned}
x_I[n] = {} & A_{IN} x_{IN}[n+\theta] \cos[2\pi(F_{BB}+F_D)(n+\theta)+\phi_1] \cdot \\
& A_{LOC} x_{LOC}[n+\overline{\theta}] \cos[2\pi(F_{BB}+\overline{F}_D)(n+\overline{\theta})+\phi_2]
\end{aligned} \tag{2}
$$

$$
\begin{aligned}
x_Q[n] = {} & A_{IN} x_{IN}[n+\theta] \cos[2\pi(F_{BB}+F_D)(n+\theta)+\phi_1] \cdot \\
& A_{LOC} x_{LOC}[n+\overline{\theta}] \sin[2\pi(F_{BB}+\overline{F}_D)(n+\overline{\theta})+\phi_2]
\end{aligned} \tag{3}
$$

where A_{LOC} is the local signal amplitude, $x_{LOC}[n]$ is the local replica of the PRN code, $\overline{F}_D$ is the local Doppler frequency shift, $\overline{\theta}$ is the local code delay and the noise has been discarded.

The obtained samples are then summed in the block called in Figure 2 as Av*erage and Dump* over one or more code periods. The correlator output for the in-phase branch can be written as

$$
\begin{aligned}
R_I[\theta,\overline{\theta},F_D,\overline{F}_D] = \sum_{n=0}^{N-1} & A_{IN} x_{LOC}[n+\theta] \cos[2\pi(F_{BB}+F_D)(n+\theta)+\phi_1] \cdot \\
& A_{LOC} x_{LOC}[n+\overline{\theta}] \cos[2\pi(F_{BB}+\overline{F}_D)(n+\overline{\theta})+\phi_2]
\end{aligned} \tag{4}
$$

and similarly for the quadrature-phase branch

$$
\begin{aligned}
R_Q[\theta,\overline{\theta},F_D,\overline{F}_D] = \sum_{n=0}^{N-1} & A_{IN} x_{LOC}[n+\theta] \cos[2\pi(F_{BB}+F_D)(n+\theta)+\phi_1] \cdot \\
& A_{LOC} x_{LOC}[n+\overline{\theta}] \sin[2\pi(F_{BB}+\overline{F}_D)(n+\overline{\theta})+\phi_2]
\end{aligned} \tag{5}
$$

The output of the envelope detector is, therefore:

$$
R_I[\theta,\overline{\theta},F_D,\overline{F}_D] = \sqrt{R_I^2(\theta,\overline{\theta},F_D,\overline{F}_D) + R_Q^2(\theta,\overline{\theta},F_D,\overline{F}_D)} \tag{6}
$$

The number of samples N depends on the sampling rate and on the so called *predetection integration time*, that is generally an integer multiple of the code period: with the increase of the integration time the complexity of the acquisition system increases and the speed of the process decreases.

In order to compare the various acquisition schemes, it is useful to evaluate their complexity: neglecting the summations and the calculation of the signal envelope and naming N_C the number of code delays to search for, N_P the number of code periods used for the non-coherent summation, $N = N_C \cdot N_P$ the total number of samples used for the integration and N_D the number of Doppler bins, the number of multiplications M required for the whole search space scanning, except the operations needed for the envelope detector, is

$$
M = N_D \cdot N_C \cdot (N + 2N) = 3N_P \cdot N_D \cdot N_C^2 \tag{7}
$$

3.2 Search scheme: 1-bit ADC with floating-point local sinusoids implementation

An implementation of the serial scheme that makes the RF front-end of the receiver less complex is shown in Figure 3: the incoming signal, after the down-conversion, is sampled with a 1-bit ADC, while the local sinusoids are floating-point signals.

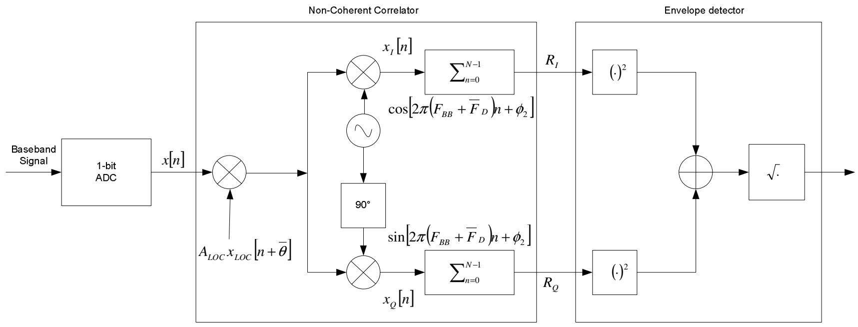

Figure 3 Serial search scheme 1-bit ADC with floating-point local sinusoids

This implementation reduces the complexity of the RF front-end, since no Automatic Gain Control is needed in order to set the correct input signal level for the ADC, and the first multiplication of the incoming signal with the replica code is very easy to implement: it can be performed through a two-by-two matrix, so it can be neglected in the complexity computation. The number of multiplications required for the scanning of the entire matrix is, therefore

$$M = N_D \cdot N_C \cdot (2N) = 2N_P \cdot N_D \cdot N_C^2 \tag{8}$$

3.3 Serial search scheme: 1-bit ADC with squared local sinusoids implementation

A third implementation of the serial search scheme uses a 1-bit ADC and local squared sinusoids, as depicted in Figure 3. The advantage of this implementation is its complexity; since all the multiplications can be performed with a two-by-two matrix and the summations use only integer values: in this case the complexity of the system is not comparable with the previous implementations and the acquisition is, therefore, much faster than the other serial search systems.

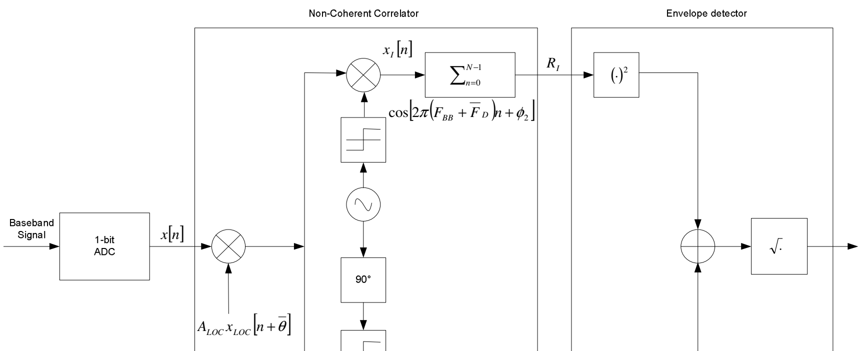

Figure 4 Serial search scheme 1-bit ADC with squared local sinusoids implementation

3.4 Parallel acquisition in time delay domain: FFT for circular correlation

The scheme shown in Figure 5 performs a parallel acquisition in time delay domain; this system is described in Tsui (2000), Nee (1991), Nee (1992) and Hyoungsoo (2000).

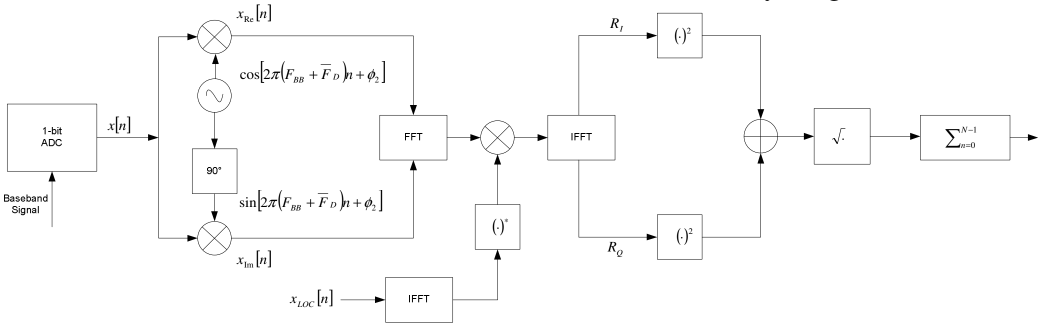

Figure 5 Parallel acquisition in time domain: FFT for circulat correlation

The acquisition method that uses the FFT for time domain parallel processing, works with a one code period long sequence. For each spreading code, a serial search in Doppler frequency domain and a parallel search in the time domain delay are performed.

The down-converted input digital signal $x[n]$ is squared by the 1-bit ADC, then it is multiplied for the sine and cosine whose frequencies are the baseband frequency plus the estimated Doppler shift; the resulting signals are the real part, $x_{\mathrm{Re}}[n]$, and the imaginary part, $x_{\mathrm{Im}}[n]$, of the FFT input. These complex samples are multiplied by the complex conjugates of the samples $X_{LOC,S}[n]$, then the inverse FFT is carried out and the absolute values of the resulting real and imaginary parts is calculated. In this way, a whole row of the search matrix, corresponding to all the possible code delays, is computed: the described operations perform the circular correlation and provide the complete correlation function over one code period.

According to Nee (1991), this acquisition system is theoretically N_P times faster than the serial search scheme, since only N_D Doppler frequency steps are needed and the N_C code delay steps are computed in parallel, but this gain is obtained only if the signal processor is fast enough to compute $K = N_P \cdot N_C$ point FFT within one dwell time.

The complexity of this acquisition system can be computed, discarding the needed operation to calculate the envelope, as

$$M = N_D N_P \left(2N_C + 2N_C \ln(N_C) + N_C\right) = N_P N_D N_C \left(2\ln(N_C) + 3\right) \qquad (9)$$

An approximate gain of about $N_C / \ln(N_C)$ is obtained with respect to the serial search scheme which uses a 1-bit ADC and floating-point local sinusoids.

3.4 Parallel acquisition in Doppler frequency domain: FFT in Doppler frequency domain

The acquisition system that performs the parallel search in the Doppler frequency domain is depicted in Figure 6: in this case the down-converted and digitized signal is multiplied with the local PRN replica code delayed of $\overline{\theta}$ and the FFT of the obtained samples is computed; the result is passed through an envelope detector and all the desired frequency step bins are investigated in parallel.

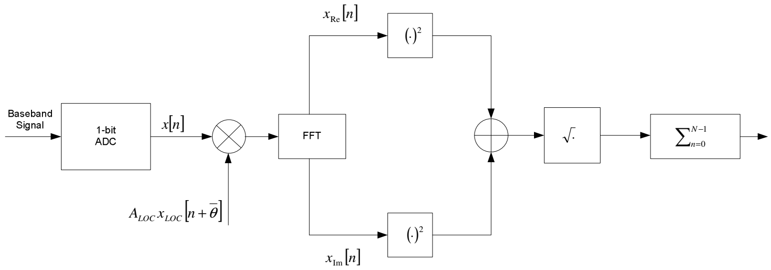

Figure 6 Parallel acquisition in Doppler frequency domain: FFT in Doppler frequency domain

The number of Doppler frequency steps and FFT points are determined by the number of code periods used for the FFT calculation: if T is the temporal duration of the input samples of the FFT, the frequency resolution is

$$\Delta\overline{f}_D = \frac{1}{T} \tag{10}$$

and the number of FFT samples depends on the sampling rate. If the sampling rate is, as usual, twice the BOC rate and the Galileo L1 code is considered, an FFT performed over one code period, ($T = 8ms$), means a number of samples equal to $N = 32736$ and a frequency resolution of $\Delta\overline{f}_D = 125Hz$.

In order to increase the SNR at the envelope detector output, two solutions are possible:

- to increase the number of code periods over which the FFT is computed equivalent to the use of more code periods in the summation of the serial search scheme,
- to compute the summation of K envelope detector output of different FFT stages, as proposed by Nee (1991).

This acquisition system requires, for each Doppler row of the serial search space, only one FFT calculation, but the whole time delay domain has to be scanned serially. The numbers of required multiplications for the entire matrix analysis, discarding the operation of the envelope detector, are

$$M = N_C \ln(N) = N_C{}^2 N_P \ln(N_C N_P) \tag{11}$$

if the non-coherent summation after the envelope detector is not used.

4. Simulation Results

Simulations have been performed in order to analyse the acquisition systems and to determine their optimum parameters. Performance are represented in terms of the so-called *Receiver Operative Characteristic*, (ROC), that is the graph of the detection probability P_d versus the false alarm probability, or, equivalently, of the missed detection probability versus the false alarm probability P_{fa}.

Both the detection and the false alarm probabilities are determined by means of the *error-counting technique*: an adequate number of samples is fed to the acquisition system in the aligned and non-aligned conditions and the number of detections in the correct bin and of false detections in the wrong bins are computed: the division of these values for the total number of used samples gives the two desired statistics.

The input signal is a baseband signal whose center frequency is $f_{BB} = 8KHz$, and the sampling rate is equal to $f_S = 4.3036MHz$. In the sampling process, the starting sampling point is a random variable which assumes values between $[0, T_C/2]$, where T_C is the chipping period. The initial phases of the received cosine and of the receiver local oscillator are random phases, uniformly distributed in the range $\phi_{1,2} = [-\pi, \pi]$. The Doppler frequency shift is in the range $f_D = [-5KHz, 5KHz]$. The simulations are performed for three input signal-to-noise ratios $SNR_{IN}\big|_{dB} = [-30, -35, -40]$.

In order to compare the three considered implementations of the serial search scheme, the ROC curves for the three systems have been computed by simulation. shows the comparison for the three SNR values (detection probability versus false alarm probability).

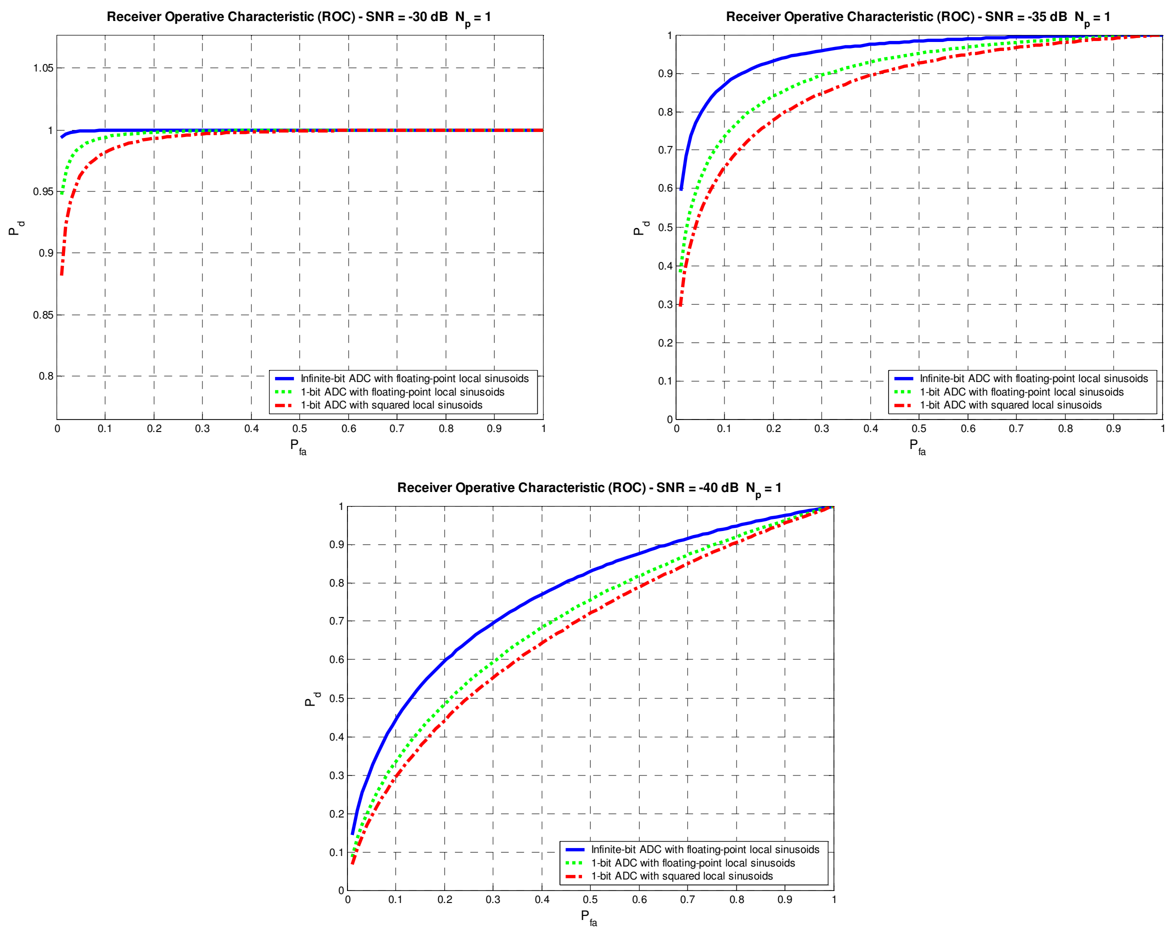

Figure 7 Comparison between the three implementation of the serial search scheme for different SNR and summation over one code period

From the previous graphs it can be noticed that most of the loss with respect to the non-quantized input signal is due to the 1-bit ADC, while a smaller loss is experienced when the squared local sinusoids are used instead of the floating-point local sinusoids. The difference between the three implementation can be better quantified by means of the graphs of Figure 8, which depicts the detection probability as a function of the signal-to-noise ratio for a desired false alarm probability equal to $P_{fa} = 10^{-3}$ in the three cases: with respect to the completely floating-point implementation, the 1-bit ADC with floating-point local signal loses $2dB$ and, with respect to this last scheme, the squared local sinusoids implementation loses another $1dB$, so that the total loss of the 1-bit ADC with squared local sinusoids scheme with respect to the infinite-bit ADC with floating-point local sinusoids is of $3dB$.

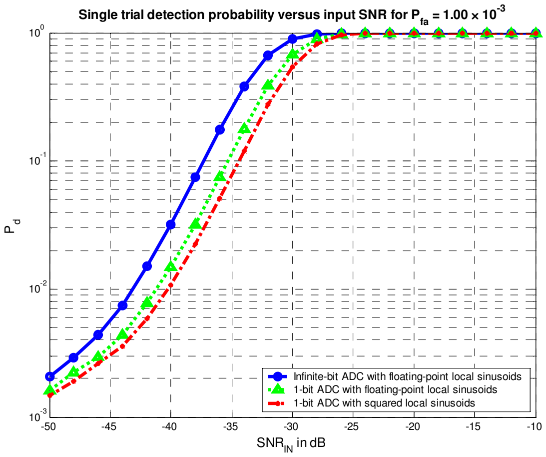

Figure 8 Comparison between the three implementation of the serial search scheme in terms of detection probability as function of the SNR for a desired false alarm probability

The loss of the 1-bit ADC implementation with respect to the non-quantized input signal system is due to the loss of information of the squared signal with respect to a signal represented with a larger number of bits; it has to be remarked that the floating-point input signal is an extreme case of ADC in which no quantization takes place, so that a real system using an ADC with a number of bits greater than one would have performance in-between these two bound. The further loss of the system that uses squared local sinusoids with respect to the system with floating-point local sinusoids, both with a 1-bit ADC, can be due to the loss of information of the squared local signals in the zero crossing points. This loss is not negligible, as can be seen from Figure 7, but it can be accepted since the 1-bit ADC with squared local signals is much less complex than the other one 1-bit ADC scheme: all the multiplications can be performed with a two-by-two matrix, so that the complexity of the two systems is not comparable.

The ROC curves can also be presented in terms of missed detection probability versus the false alarm probability, as shown in Figure 9 for the completely floating-point implementation and in Figure 10 for the completely squared implementation.

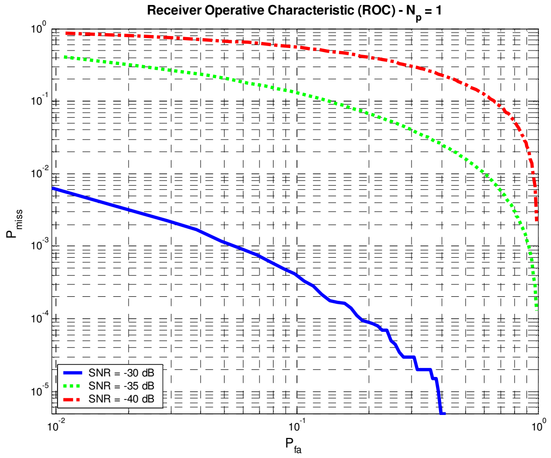

Figure 9 Infinite bit ADC with floating point local sinusoids implementation

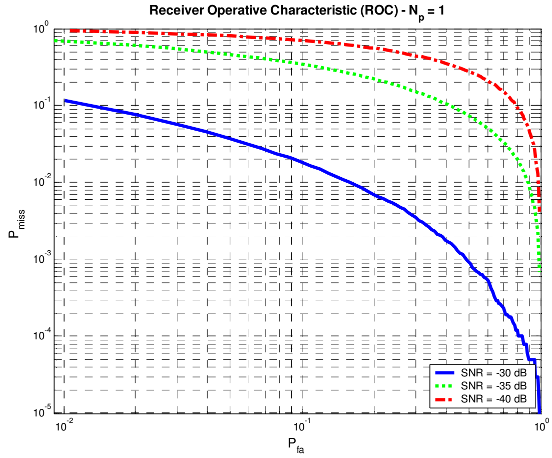

Figure 10 1 bit ADC with squared local sinusoids implementation

The simulated ROC curves for the three considered signal-to-noise ratios and for the FFT in Doppler frequency domain scheme performed over one BOC(1,1) code period are shown, in Figure 11.

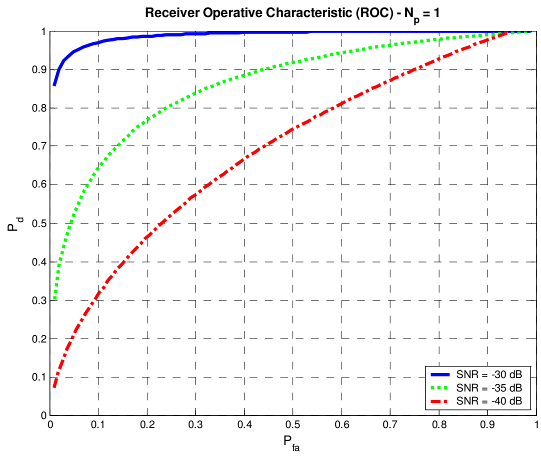

Figure 11 ROC Curves for one code period FFT input and for different SNR

In order to compare the FFT acquisition technique with the serial search system, the graphs of Figure 12 shows the ROC curves for the completely floating--point serial search scheme, the completely squared serial search technique and the FFT acquisition scheme. The performances of this last scheme are better than the completely squared serial search scheme, and intermediate between the two other systems.

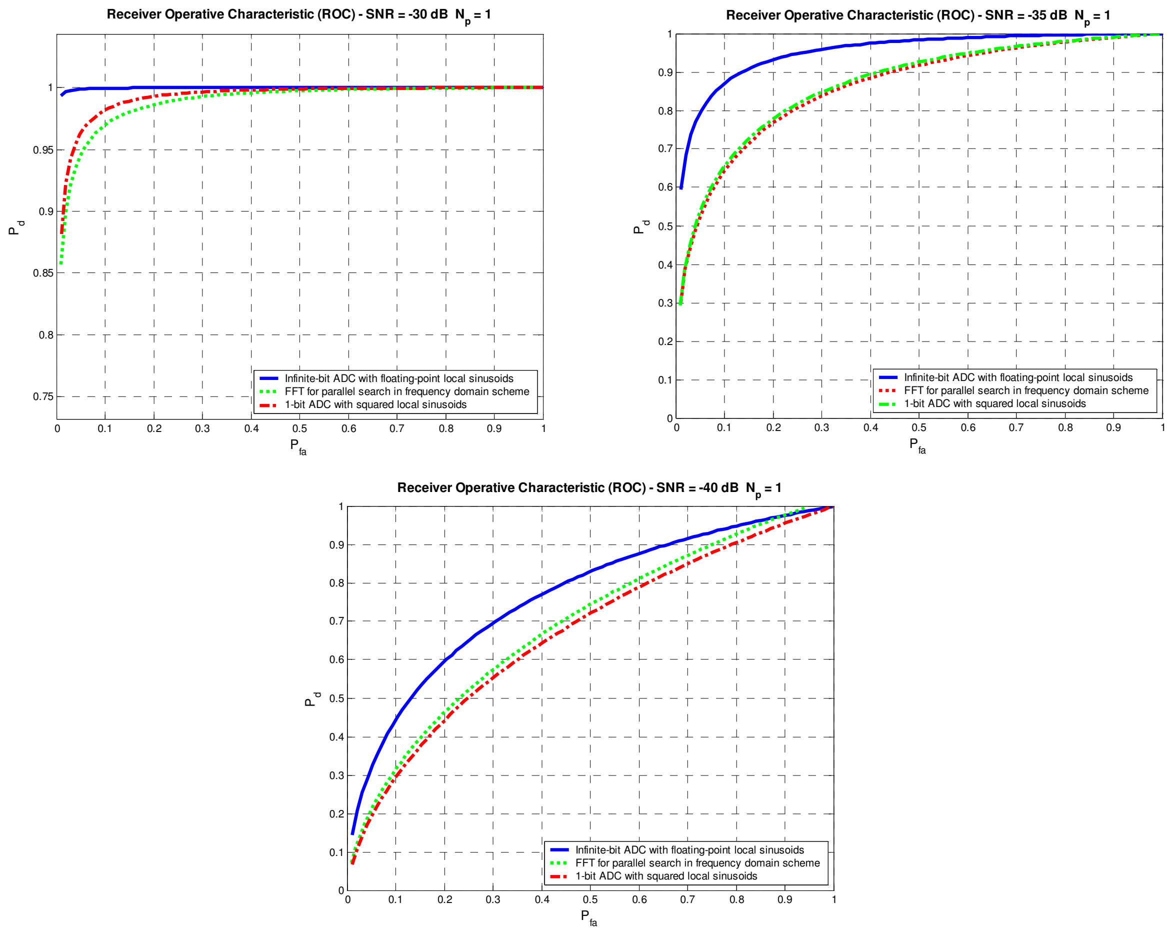

Figure 12Comparison between ROC curves for the FFT acquisition system, the complete floating point serial search system and the complete squared serial search scheme

3. Conclusions

In this paper a comparison between several acquisition schemes has been performed considering the Galileo OS signals.

The best performance can be obtained with the complete floating point serial search, which is more complex than the quantized scheme. From the performed analysis, it can be derived that the serial search scheme with a 1-bit ADC and squared local sinusoids shows slightly worse performances than the FFT technique which carries out a parallel search in frequency domain, if the number of processed code periods is the same, but it results to be less complex.

The FFT scheme, in fact, requires a DSP which computes one FFT of complex samples for each code phase delay, while in the completely squared system all the multiplications can be carried out through a two-by-two matrix.

In the serial search system, besides, the Doppler frequency step width can be set to the most suitable value, while in the FFT scheme the frequency resolution is determined by the FFT itself and cannot be modified.

ACKNOWLEDGEMENTS: Maurizio Fantino would like to thank Alenia Spazio- Laben, that is sponsoring his Ph.D grant.

REFERENCES

Betz JW (1999), ***The Offset Carrier Modulation for GPS Modernization***, Institute of Navigation – NTM, San Diego, CA, 639-649.

Chang HS, Park YW and Lee YH (2000), ***Ds-ss code acquisition based on simulataneous search and verification***, IEEE Trans. Commun, 48, 921-924.

Delva J and Howitt I (2001), ***A coherent acquisition method for a pn sequence using binary search and an auxiliary sequence***, IEEE J. Select. Areas Commun, 48, 2432-2440.

Hopkins P (1997), ***A unified analysis of pseudonoise synchronization by envelope correlation***, IEEE Trans. Commun, 25, 770-778.

Holmes J and Chen C (1997), ***Acquisition time performance of pn spread spectrum system***, IEEE Trans. Commun, 25, 778-784.

Holmes J and Chen C (1997), ***Acquisition of pseudonoise signals by recursion aided sequential estimation***, IEEE Trans. Commun, 25, 784-794.

Hyoungsoo L, Lee SI and Lee SP (2000), ***A simple carrier frequency detection algorithm for fine compensation of Doppler shift in direct-sequence code division multiple access mobile satellite communications***, IEEE Proceedings of International Conference on Communication, 1, 109-112.

Lee S and Kim J (2001), ***Effects of multiple threshold values for pn code acquisition in ds-cdma system***, Electronics Letters, 6, 363-365.

Nee DV and Coenen A (1991), ***New fast gps code-acquisition technique using low fft***, Electronics Letters, 27, 158-160.

Nee DV and Coenen A (1991), ***Novel fast gps/glonass code acquisition techniques using low update rate fft***, Electronics Letters, 28, 863-865.

Polydoros A and Weber C (1984), ***A unified approach to serial search spread spectrum code acquisition –part I, General theory***, IEEE Trans. Commun, 32, 542-549.

Polydoros A and Weber C (1984), ***A unified approach to serial search spread spectrum code acquisition –part II, General theory***, IEEE Trans. Commun, 32, 550-560.

Rappaport S and Grieco D (1984), ***Spread Spectrum signal acquisition: Methods and technology***, IEEE Commun. Mag, 22, 6-21.

Tae-Hoon K, Kyung-Woom J and Yong-Wan P (2000), ***Effects of multiple threshold values for pn code acquisition in ds-cdma system***, Electronics Letters, 1, 660-664.

Tsui JBY (2000), ***Fundamental of Global Positionins System Receivers. A Software Approach***, New York: John Wiley and Sons.

Weihua Z and Tranquilla J (1995), ***Modeling and analysis for the gps pseudo-range observable***, IEEE Trans on Aerosp. Electron. Syst, 31, 739-751.

Yan L, Yuchu M and Zhongzhao Z (2002), ***Modified non-coherent sequential acquisition scheme of ds/ss signals***, IEEE Proceeding. of the 3rd International Conference on 3G Mobile Communication Technologies, 489, 160-164.